

# A PAH Deficit in Extremely Low Luminosity Galaxies

Ronin Wu<sup>1</sup>, David W. Hogg<sup>1</sup>, and John Moustakas<sup>1</sup>

## ABSTRACT

Low levels of polycyclic hydrocarbon (PAH) emission in the spectra of dwarf galaxies has been a puzzle for the past 20 years. Here, we present the mid-infrared (MIR) properties of 27 extremely low luminosity dwarf galaxies ( $M_r > -15$  mag) observed with the Spitzer Infrared Array Camera (IRAC). The dwarf galaxies studied in this work are randomly selected from the Sloan Digital Sky Survey (SDSS). They are nearby ( $z \lesssim 0.005$ ) and are mostly isolated from more luminous galaxies. Using the magnitude at  $7.8\mu\text{m}$  as a tracer of PAH content and the magnitude at  $3.6\mu\text{m}$  as a tracer of stellar population, we compare the  $[7.8\mu\text{m}]-[3.6\mu\text{m}]$  color with metallicity based on oxygen and nitrogen lines, and  $\log([\text{OIII}]/\text{H}\beta)$ , which is used as an indicator of radiation field hardness. We find that the PAH feature in the  $7.8\mu\text{m}$  band becomes weaker as the total galaxy luminosity becomes fainter. This is in agreement with earlier observations of dwarf galaxies, including a small sample taken by ISO, and the data taken from overlap of SDSS with the Spitzer First Look Survey. This work contains galaxies of mean absolute magnitudes about 3 mags fainter than any previously studied sample of dwarf galaxies.

*Subject headings:* galaxies: dwarf — galaxies: evolution — galaxies: ISM — infrared: galaxies — ISM: general

## 1. Introduction

Star formation in galaxies is closely related to dust and gas contents. Interstellar dust grains and molecules, excited by ultraviolet (UV) photons emitted by young stars, reemit photons usually in the mid-infrared (MIR). The spectra of star-forming galaxies in MIR are generally dominated by five prominent features at 3.3, 6.2, 7.7, 8.6 and  $11.3\mu\text{m}$ . These features, once known as Unidentified Infrared Bands (UIB), are now commonly attributed to the small ( $5\text{\AA}$ ) PAH grains. These features are optical-vibrational modes of molecules

---

<sup>1</sup>Center for Cosmology and Particle Physics, Department of Physics, New York University

excited by UV stellar light and are found in a wide variety of systems (Leger and Puget 1984; Allenmandola et al. 1989; Tielens et al. 1999).

Interest in the PAH emission from low-luminosity systems arose from observations of NGC 5253 and II Zw 40 (Roche et al. 1991). The PAH features are absent from the spectra of these two starburst dwarf galaxies despite large star-formation rates. The PAH deficit in low-luminosity systems has been confirmed with SBS 0335-052; despite very strong star formation activity, the PAH features were absent from its MIR spectrum (Thuan et al. 1999; Dale et al. 2001; Houck et al. 2004). Detailed studies of individual star-forming dwarf galaxies, e.g., blue compact dwarf galaxies (BCDs) generally show suppressed PAH emission (Jackson et al. 2006; Wu et al. 2006). Analyses of dwarf galaxies selected from Spitzer’s Infrared Array Camera (IRAC) observations and Sloan Digital Sky Survey (SDSS) (York et al. 2000) and KPNO International Spectroscopic Survey (KISS, Salzer et al. 2000) find that dwarf galaxies generally have weaker PAH emission when compared to the normal star-forming galaxies of similar optical color (Hogg et al. 2005; Rosenberg et al. 2006; Wu et al. 2007). By comparing optical spectra of dwarf galaxies with normal star-forming galaxies, here we examine the relationship of PAH emission with metallicity and radiation hardness.

## 2. Results

We classify our galaxies into two groups based on the Baldwin-Phillips-Terlevich diagram (Baldwin et al. 1981, hereafter BPT diagram). By plotting  $\log([\text{O III}]/\text{H}\beta)$  (hereafter “O3”) as a function of  $\log([\text{N II}]/\text{H}\alpha)$  (hereafter “N2”), we classify all the galaxies into star forming galaxies and active galactic nuclei (AGN). The line emission data for the SWIRE/SDSS galaxies is taken from the public data contributed by the research groups from Max-Planck Institute for Astrophysics and Johns Hopkins University<sup>2</sup>. The line emission data for the FLS/SDSS galaxies, the galaxies taken from Rosenberg et al. (2006) and the 27 extremely low luminosity galaxies are obtained by fitting the SDSS spectra with the population synthesis model established by Bruzual and Charlot (2003) and Tremonti et al. (2004). The demarcation determined by Kauffmann et al (2003) separates AGN galaxies from star forming galaxies in Fig.(1).

For star-forming galaxies, the emission received by the fourth channel of IRAC at  $7.8\mu\text{m}$  is dominated by a PAH feature at  $7.7\mu\text{m}$ . Since the first channel ( $3.6\mu\text{m}$ ) of IRAC is at the Rayleigh-Jeans limit of a blackbody spectrum for starlight with  $T > 2000\text{K}$ , we can use this channel as a direct tracer of both early and late type stellar mass distributions

---

<sup>2</sup><http://www.mpa-garching.mpg.de/SDSS>

free of dust obscuration effects (Pahre et al. 2004). Subtraction of the two magnitudes,  $[3.6\mu\text{m}]-[7.8\mu\text{m}]$  (hereafter “PAH/star”), therefore, can be used to indicate the mean PAH emission per unit stellar mass.

Fig.(2) shows how PAH/star depends on optical  $g - r$  color for star-forming galaxies. Normal star-forming galaxies with  $M_r < -19$  mag generally lie on a trend with red (old) galaxies showing low PAH/star and blue (young) galaxies showing high PAH/star. Since PAH emission is mainly produced by absorption of UV photons emitted by massive stars (Li and Draine 2002; Peeters et al. 2004), red galaxies, which are lacking young massive stars, are incapable of producing high PAH emission. On the other hand, blue galaxies, still young and actively star forming, have massive stars that are capable of exciting the PAH molecules. At the bluer end ( $g - r \lesssim 0.6$  mag), the PAH/star value decreases as optical luminosity ( $M_r$ ) becomes fainter even though the optical color remains blue. This deviation of low luminosity systems from the main trend of PAH/star versus optical color was also discussed in Hogg et al. (2005) and Rosenberg et al. (2006). With the extremely low luminosity galaxies ( $M_r > -15$  mag) plotted in Fig.(2), it is clear that the PAH emission in dwarf galaxies is strongly suppressed. The cause of this suppression is possibly a mixture of various factors, including possibly young age, low metallicity, or hard radiation field (O’Halloran et al. 2006; Wu et al. 2006). Here, we investigate these possibilities.

## 2.1. PAH/star and Metallicity

Dwarf galaxies are low in metallicity. It is possible that the metal-poor environment in dwarf galaxies makes it difficult for the synthesis of PAH grains (Engelbracht et al. 2005; Madden et al. 2006; Rosenberg et al. 2006; Wu et al. 2006).

Our result in Fig.(3) shows a strong correlation between PAH/star and metallicity  $12 + \log(O/H)$ . Our estimate of the metallicity is based on the O3N2 parameter (Eq.1) defined in Pettini et al. (2004).

$$O3N2 = \log\left(\left(\frac{[O\text{III}]/H\beta}{[N\text{II}]/H\alpha}\right)^2\right) \quad (1)$$

The data presented in Fig.(3) excludes all galaxies with  $S/N < 3$  in  $H\alpha$ ,  $[O\text{ III}]$ ,  $[N\text{ II}]$ , and  $H\beta$ . This cut leaves 372 star forming galaxies in total. The median  $12 + \log(O/H)$  of the low luminosity galaxies studied in this work is 7.65 ( $\sim Z_{\odot}/20$ , with  $Z_{\odot}$  calculated from Allende Prieto et al. 2001).

As PAH/star value decreases, the measured value of metallicity distributes over a wider region ( $\sim 1.5$ dex). This increased uncertainty in metallicity-PAH/star relationship observed

for low PAH/star (PAH/star  $\leq 0$ ) galaxies is partly caused by the uncertainty in the applicability of the linear relation between O3N2 and  $12 + \log(O/H)$  for low metallicity systems. The relation between  $12 + \log(O/H)$  and O3N2 has uncertainty greater than  $\sim 0.25$  when  $12 + \log(O/H) < 8.1$  (Pettini et al. 2004).

## 2.2. PAH/star and Radiation Hardness

The absence of emitting PAHs in dwarf galaxies can also be a consequence of PAH destruction by hard ultraviolet(UV)-photons. It was noted that PAH features are absent from AGN spectra (Aitken and Roche 1985). The relationship between PAH strength and [NeIII]/[NeII], an indicator of radiation hardness, indicates that PAH features are generally suppressed as the radiation field gets harder in star forming galaxies (Madden et al. 2006; Wu et al. 2006).

In our analysis, we use  $O3 = \log([OIII]/H\beta)$  as an indicator for radiation hardness. Fig.(4) shows PAH/star as a function of O3 for 372 star forming galaxies with  $S/N \geq 3$  in  $H\alpha$ , [O III], [N II], and  $H\beta$ . Galaxies with very low luminosities ( $M_r > -17$  mag) are generally found at  $O3 > 0$  and PAH/star  $< 0$ . This trend implies that suppression of PAH emission in dwarf galaxies can be due to the destruction of PAH molecules near hard-UV radiation sources.

## 3. Conclusion

We present MIR properties of 27 extremely low luminosity galaxies with  $M_r > -15$  mag based on Spitzer IRAC observations. Comparing with normal star forming galaxies ( $M_r < -17$  mag), these galaxies appear to be bluer in  $g - r$  color when observed with SDSS, and they also show bluer [7.8  $\mu\text{m}$ ]-[3.6  $\mu\text{m}$ ] color (PAH/star). Metallicity calculated based on oxygen and nitrogen lines is 7.65 ( $\sim Z_{\odot}/20$ , with  $Z_{\odot}$  calculated from Allende Prieto et al. 2001) at median for the 27 dwarf galaxies studied in this work. PAH emission is generally suppressed in these metal-poor galaxies. Our analysis shows that PAH/star in star forming galaxies increases with metallicity and decreases with radiation hardness. This indicates that the suppression of PAH in dwarf galaxies can be due the mixture of their low metallicity and hard radiation fields, but certainly does not rule out other causes, since many galaxy properties are related to metallicity and radiation fields.

## REFERENCES

- Abazajian, K. et al. 2004, AJ, 128, 502
- Aitken, D. K. and Roche, P. F. 1985, MNRAS, 213, 777
- Allende Prieto, C. et al. 2001, ApJ, 556, L63
- Allenmandola, L. J. et al. 1989, ApJS, 290, L25
- Baldwin, J. et al. 1981, PASP, 93, 5
- Bruzual, G., Charlot S. 2003, MNRAS, 344, 1000
- Dale, D. A. et al. 2001, AJ, 122, 1736
- Elbaz, D. et al. 2005, A&A, 434, L1
- Engelbracht, C. W. et al. 2005, ApJ, 628, L29
- Fazio, G. G. et al., 2004, ApJS, 154, 10
- Hogg, D. W. et al., 2005, ApJ, 624, 162
- Houck, J. R. et al., 2004, ApJS, 154, 211
- Izotov, Y. I. et al., 1997, ApJ, 476, 698
- Jackson, D. C. et al., 2006, ApJ, 646, 192
- Kauffmann, G. et al., 2003, MNRAS, 346, 1055
- Leger, A. and Puget, J. L., 1984, ApJ, 137, L5
- Li, A. and Draine, B. T., 2001, ApJ, 554, 778
- Li, A. and Draine, B. T., 2002, ApJ, 572, 232
- Madden, S. C. et al., 2006, A&A, 446, 877
- O’Halloran, B. et al., 2006, ApJ, 641, 795
- Pahre, M. A. et al., 2004, ApJS, 154, 235
- Pettini, M. and Pagel, B. E. J., 2004, MNRAS, 348, L59
- Peeters, E., Spoon, H. W. W., and Tielens, A. G. G. M., 2004, ApJ, 613, 986

- Roche, P. F. et al., 1991, MNRAS, 248, 606
- Rosenberg, J. L. et al., 2006, ApJ, 636, 742
- Rosenberg, J. L. et al., 2007, arXiv:0710.5514
- Salzer, J. J. et al., 2000, AJ, 120, 80
- Surace, J. A. et al., 2005, Spitzer Science Team, California Institute of Technology
- Thuan, T. X., Sauvage, M and Madden, S., 1999, ApJ, 516, 783
- Tielens, A. G. G. M. et al., 1999, ESA SP-427, 579
- Tremonti, C. A. et al., 2004, ApJ, 613, 898
- Werner, M. et al., 2004, ApJS, 154, 1
- Wu, Y. et al., 2006, ApJ, 639, 157
- Wu, H. et al., 2007, ApJ, 668, 87
- York, D. et al., 2000, AJ, 120, 1579

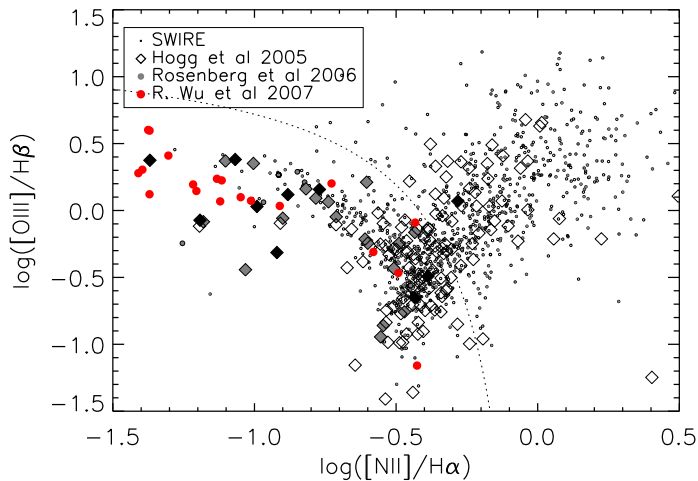


Fig. 1.— The Baldwin-Phillips-Terlevich (BPT) diagram (Baldwin et al. 1981) of galaxies studied in this work. The distribution of  $\log([\text{O III}]/\text{H}\beta)$  versus  $\log([\text{N II}]/\text{H}\alpha)$  is used to distinguish type 2 AGNs from normal star-forming galaxies. The dotted line is the demarcation curve fitted by Kauffmann et al (2003). This curve separates star-formation galaxies (below) from AGNs (above).

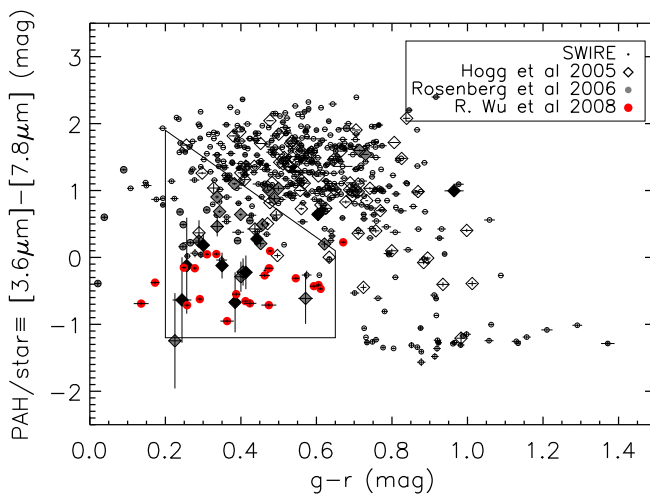


Fig. 2.— The distribution of PAH/star versus optical  $g-r$  color for star forming galaxies selected with Fig.(1).  $g-r$  colors are calculated in AB system. The symbol scheme used here except for the 27 extremely faint galaxies is as follows: open symbols are galaxies brighter than  $M_r = -19.0$  mag, the grey ones are galaxies with  $-19.0 \leq M_r < -17.0$  mag, and the black ones are galaxies fainter than  $M_r = -17.0$  mag..

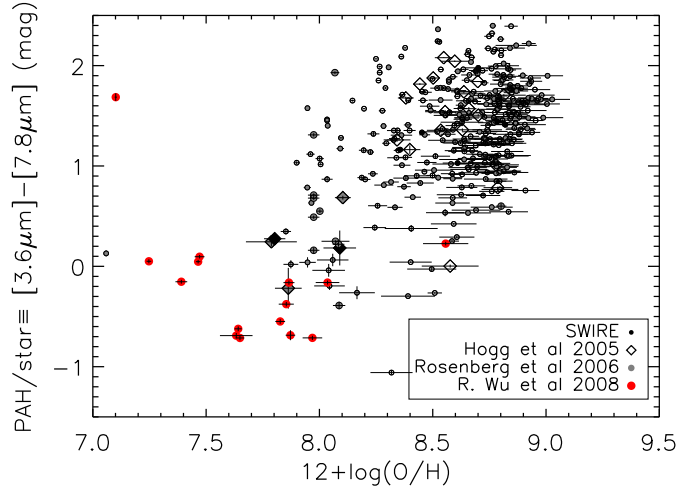


Fig. 3.— The relationship between PAH/star and metallicity for star-forming galaxies. The metallicity is calculated based on oxygen and nitrogen lines as fitted by Pettini et al. (2004). The symbol scheme used here is as described in Fig.(2). The median metallicity of our sample is  $\sim 7.65$ .

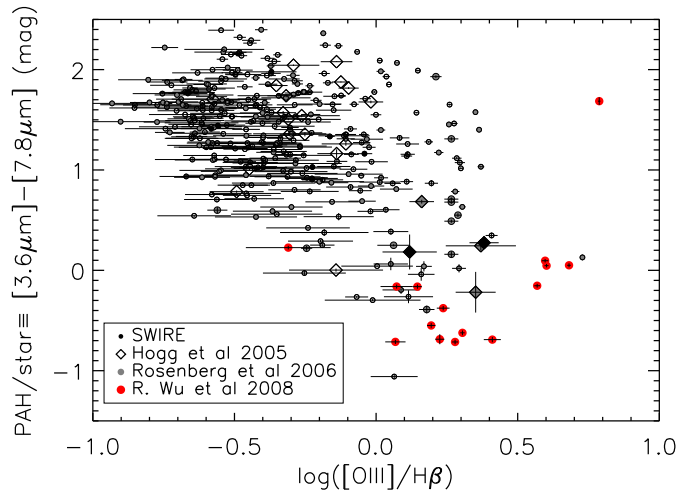


Fig. 4.— The relationship between PAH/star and radiation hardness of the starburst galaxies. The radiation strength is indicated by  $O3 = \log([\text{OIII}]/\text{H}\beta)$  on this plot. The symbol scheme used here is as described in Fig.(2).